Stellar Populations in the Milky Way and Beyond
Proceedings IAU Symposium No. 395, 2026
J. Meléndez, C. Chiappini, R. Schiavon & M. Trevisan, eds.
doi:10.1017/S174392132500170X

Multiple Populations in Massive Clusters

Carmela Lardo

Dipartimento di Fisica e Astronomia "Augusto Righi"-Università di Bologna, via Piero Gobetti 93/2, I-40129 Bologna, Italy

INAF - Osservatorio di Astrofisica e Scienza dello Spazio di Bologna, via Piero Gobetti 93/3, I-40129 Bologna, Italy

Abstract. The first observations of light-element variations in massive clusters—commonly referred to as multiple populations—were made over 40 years ago. Despite significant advancements in spectroscopic and photometric data in recent years, which have provided highly detailed observational insights into multiple populations in clusters within the local universe, we still lack a comprehensive quantitative framework to fully explain the origin of these chemical peculiarities.

In this review, I briefly summarize the observational evidence gathered on multiple populations, their characteristics, and their trends with cluster parameters. Additionally, I highlight recent findings—both observational and theoretical—that hold great promise for understanding the origin of multiple populations and, ultimately, the processes driving star formation in massive clusters.

Keywords. globular clusters: general, stars: population II, stars: abundances

1. Introduction

Two major discoveries in recent years have significantly challenged the traditional view of globular clusters (GCs) as homogeneous, ancient fossils from the earliest stages of galaxy formation. First, observations of starburst and merging galaxies have revealed young massive star clusters whose sizes, luminosities, and colours suggest they could be newly formed globular clusters (e.g. Portegies Zwart, McMillan, & Gieles 2010). Additionally, evidence has shown that many–perhaps all–GCs host two or more distinct subpopulations of stars, each with significantly different chemical compositions (e.g. Bastian & Lardo 2018). These multiple populations (MPs) in GCs are characterized by variations in He, several light elements (C, N, O, Na, Mg, Al), and, in some cases, even iron (Gratton et al. 2004, 2012, 2019; Milone & Marino 2022).

The widely accepted explanation for the origin of MPs involves sequential star formation events during the cluster's early evolution. In this framework, the first bf population of stars (P1) forms with primordial compositions. Subsequently, a second population (P2) emerges, characterized by enhanced abundances of He, N, and Na. These P2 stars are thought to form from the processed ejecta of massive first-generation stars—such as rotating massive stars, asymptotic giant branch (AGB) stars, interacting binaries, supermassive and very massive stars, and red supergiants—mixed to varying degrees with unprocessed gas (e.g., Decressin et al. 2007; D'Ercole et al. 2010; D'Antona et al. 2016; Renzini et al. 2022). This interpretation is primarily based on observed correlations and anti-correlations in light-element abundances, commonly attributed to high-temperature CNO processing. Specifically, all the proposed stellar sources are sufficiently massive to reach the high temperatures required to produce Na (T > 40 MK) and deplete Mg (T > 70 MK; Charbonnel 2016).

© The Author(s), 2026. Published by Cambridge University Press on behalf of The International Astronomical Union. This is an Open Access article, distributed under the terms of the Creative Commons Attribution licence (https://creativecommons.org/licenses/by/4.0/), which permits unrestricted re-use, distribution and reproduction, provided the original article is properly cited.

https://doi.org/10.1017/S174392132500170X Published online by Cambridge University Press

While this scenario resembles typical self-enrichment processes, the MP phenomenon is unique because GCs remain homogeneous in their iron content. Typically, any spread in [Fe/H] is limited to a small variation of ∼0.1 dex among P1 stars (Marino et al. 2019a; Legnardi et al. 2022; Lardo et al. 2022, 2023). This implies that P2 must form before the majority of core-collapse supernovae (CCSNe), posing the so-called "supernova avoidance problem" (Renzini et al. 2015).

Despite considerable effort from the community, the origin of MPs remains unresolved. Current theoretical models, including those suggesting that second-generation stars form from the ejected material of a prior generation, face significant challenges (Bastian & Lardo 2018). These models struggle to reconcile with an expanding body of empirical evidence, highlighting the need for a paradigm shift or fresh insights into the origins of MPs (see, e.g., Bastian et al. 2015; Kruijssen 2015; Larsen et al. 2012; Renzini 2008; Renzini et al. 2015; Renzini 2017; Renzini et al. 2022, for detailed critiques).

2. A Brief Overview of the Observational Framework

Over the years, the problem of MPs has attracted the attention of many researchers, resulting in a vast amount of data being collected. Spectroscopic studies have played a crucial role, providing detailed insights not only into individual clusters but also through homogeneous data from large-scale surveys. Notable examples include APOGEE (Mészáros et al. 2015; Masseron et al. 2019; Schiavon et al. 2017, 2024), the Gaia-ESO survey (Pancino et al. 2017), the FLAMES Survey of Southern GCs led by Carretta and collaborators (Carretta et al. 2009, 2010), and the comprehensive survey of Northern clusters conducted by the Lick-Texas group (e.g., Kraft et al. 1995; Sneden, Pilachowski, & Kraft 2000; Sneden et al. 2004; Ivans et al. 2001).

However, in recent years, photometry has really given fresh momentum to the study of MPs. This is because with photometry we can observe a large number of stars over wide radial distances from the cluster centre within relatively short observation times. This efficiency allows to leverage extensive statistical datasets to better understand the properties of MPs and explore their correlations with other parameters (e.g., Monelli et al. 2013; Stetson et al. 2019; Bonatto et al. 2019; Kader et al. 2023).

A prime example is the Hubble Space Telescope (HST) *UV* Legacy Survey of Galactic Globular Clusters (HUGS; Piotto et al. 2015; Soto et al. 2017), which has delivered a comprehensive view of MPs in 57 old (≥10 Gyr) Galactic GCs. This survey complemented optical data from the ACS Survey of Galactic GCs (Sarajedini et al. 2007) with *UV* observations using HST filters that are highly sensitive to MPs (see Fig. 1).

Its success came through the introduction of the chromosome map (CMs; Milone et al. 2015, 2017; a diagnostic tool that uses fluxes from the $F275W$, $F336W$, $F438W$, and $F814W$ filters to distinguish between subpopulations with distinct chemical compositions (Fig. 2). In these maps, stars separate into P1 and P2 populations when stars with available spectroscopic data are plotted in the colour-colour space (Marino et al. 2019a). P1 stars, characterized by a "field-like" composition, cluster in the lower-right corner of the CM, while P2 stars exhibit a more elongated distribution extending toward the upper-left corner (see Milone et al. 2017, for a collection of CMs in Galactic GCs).

Chromosome maps thus provide an efficient means of characterizing the range of light-element variations in the HUGS survey. However, they also reveal that the chemical variations underlying the MP phenomenon may be more complex than previously thought. Notably, some clusters exhibit unexpected colour spreads among P1 stars (Lardo et al. 2018; Milone et al. 2018), which suggest a metallicity variation within this group (Marino et al. 2019b; Legnardi et al. 2022; Lardo et al. 2022, 2023), a feature not accounted for by traditional MP models.

https://doi.org/10.1017/S174392132500170X Published online by Cambridge University Press

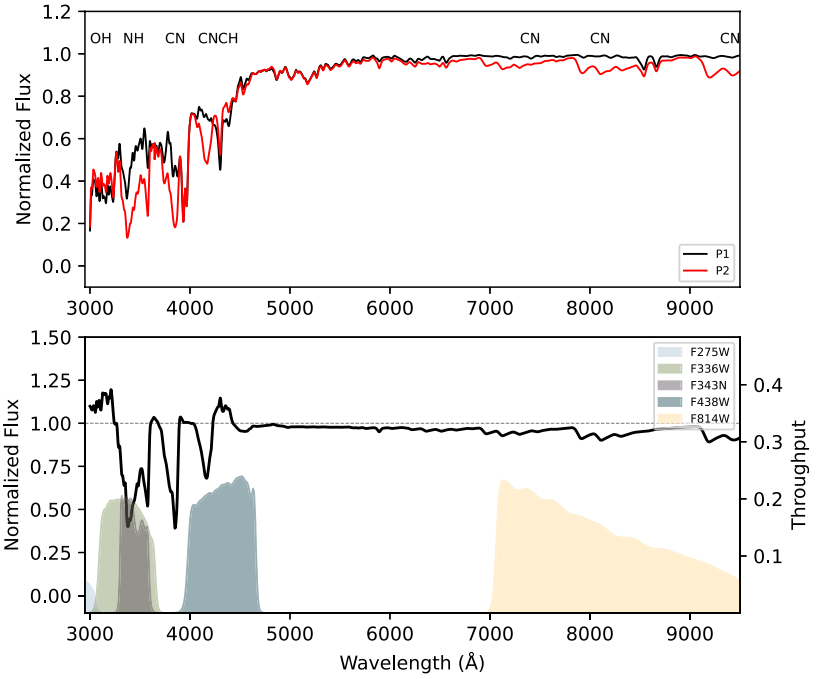


Figure 1. In the top panel, the black line represents the spectrum of a red giant star (RGB) with a typical P1 composition, while the red line shows the spectrum of a star with P2 chemistry but identical stellar parameters. The lower panel illustrates the ratio of these fluxes, clearly highlighting significant variations at wavelengths shorter than 4000 Å , where numerous NH, CN, and CH absorption features are present. This implies that constructing a colour-magnitude diagram (CMD) using a *U*-based filter would reveal a broadened red giant branch—exceeding what can be explained by photometric errors alone. In some cases, discrete sequences may also emerge, particularly if N variations are present. The throughput of HST filters commonly used to investigate MPs is also shown for reference.

Furthermore, certain clusters contain stars that extend to the upper-right corner of the CM, exhibiting typical C-N and Na-O anti-correlations along with enhanced C+N+O sums and increased slow neutron-capture process element abundances (Marino et al. 2012). The origin of this additional population remains a subject of active debate, with no fully satisfactory explanation currently available.

2.1. *Observed Trends with Mass*

A challenge with MP models that was recognized early on is the so-called *mass budget* problem (de Mink et al. 2009; Gratton et al. 2012; Kruijssen 2015). Since second-generation (P2) stars typically outnumber first-generation (P1) stars (Carretta et al. 2010; Milone et al. 2017), the amount of material processed by massive first-generation stars would be insufficient to account for the observed P2/P1 ratios—unless extreme assumptions are made about star formation efficiency, the initial mass function, or the preferential loss of first-generation stars. To address this issue, the prevailing solution has been to propose that GCs were 10-100 times more massive at birth. This scenario creates a sufficiently large reservoir of gas, enriched with CNO-burning products, to explain the observed population ratios.

While it is certainly true that GC systems formed with much more mass than is observed today, this universal mass loss is not expected from models of GC evolution;

https://doi.org/10.1017/S174392132500170X Published online by Cambridge University Press

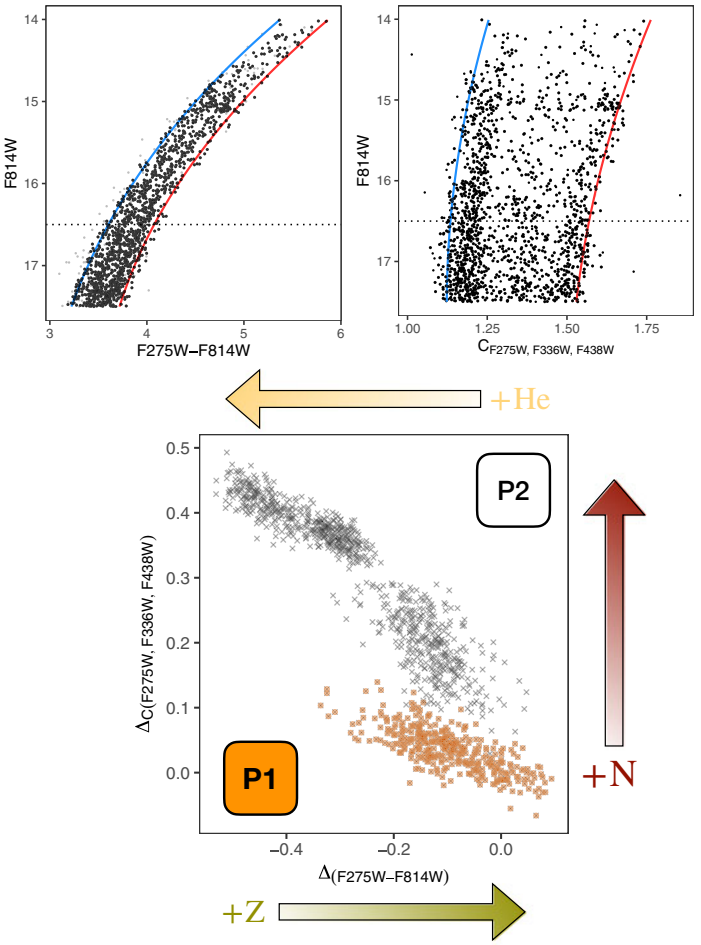


Figure 2. This figure summarizes the construction of CMs, as presented in Milone et al. (2017). In the top two panels, the RGBs of the surveyed clusters are plotted in the $F275W - F814W$ vs. $F814W$ and $C_{\rm F275W,\ F336W,\ F438W} = (F275W - F336W) - (F336W - F814W)$ vs. $F814W$ CMDs. The latter colour combination is similar to the c_y color index introduced by Yong et al. (2008) using Strömgren photometry, as well as the $CUBI$ index from ground-based photometry (Monelli et al. 2013). These plots effectively highlight the separation of discrete photometric sequences corresponding to stars with different chemical compositions. In particular, the broad baseline of the $F275W - F814W$ colour combination accentuates temperature differences among stars, allowing for the distinction—at least in a first approximation—between stars with varying He content and/or metallicity. The $C_{\rm F275W,\ F336W,\ F438W}$ index is particularly sensitive to N variations. Colour spreads in the two colour combinations are calculated relative to the ridge lines along the RGB, effectively *verticalising* the sequence. These spreads are then normalized using the width of the RGB at a given luminosity above the turn-off, shown as a dotted horizontal line in the figure (see Milone et al. 2017, for a discussion). Finally, the two color spreads are plotted against each other to create the CM shown in the lower panel. In this diagram, distinct groups of stars—each occupying a specific position based on their chemical composition—are clearly identifiable. As a result, P1 stars are separated from second-population stars. The arrows on the map illustrate how variations in He, N, and overall metallicity (Z) influence the positions of individual stars.

https://doi.org/10.1017/S174392132500170X Published online by Cambridge University Press

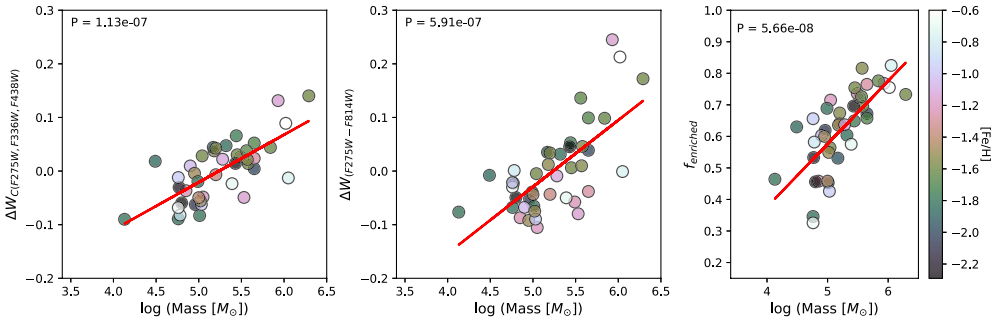


Figure 3. The figure summarizes how the properties of MPs vary with the present-day mass of GCs. These results are derived from the HUGS survey, as reported in Milone et al. (2017). The quantities $\delta W_{C(F275W,F336W,F438W)}$ and $\delta W_{F275W-F814W}$ represent the widths of the RGB in two different colour combinations (cf. Fig. 2), corrected for metallicity effects. To a first approximation, these widths are positively correlated with the levels of N and He enrichment, respectively, within cluster stars. The fraction of P2 stars relative to the total number of stars on the RGB is denoted as $f_{\rm enriched}$. The left and middle panels clearly demonstrate that both colour spreads are positively correlated with the present-day mass of the cluster. The right-hand panel illustrates the relationship between $f_{\rm enriched}$ and cluster mass. The red solid lines in each panel represent the best linear fit to the data, with the corresponding probability (P) of no correlation between the points provided. Clusters are colour-coded according to their metallicity. All data are sourced from Milone et al. (2017).

instead, it comes from extreme fine-tuning of the initial conditions. Additionally, this assumption is in tension with the observed properties of the present-day GC population (e.g. Conroy 2012; Kruijssen 2015; Bastian et al. 2015), the metallicity distributions of cluster and field stars in dwarf galaxies (Larsen et al. 2012, 2014), and the specific frequency of GC systems in galaxies (Kruijssen 2015).

Finally, the strong correlation between present-day GC mass and the fraction of P2 stars, as well as the extent of the chemical ranges between the populations (e.g., Carretta et al. 2010; Schiavon et al. 2013; Milone et al. 2017, 2018, see Fig. 3.); also argues against scenarios that invoke extreme mass loss. Dynamical cluster disruption mechanisms are in fact not capable of explaining the high-enriched fractions observed in GCs nor their positive trend with cluster mass (e.g. Reina-Campos et al. 2018).

Taken together, these observations suggest that *(a)* the physical mechanism responsible for the presence of MPs is likely dependent on the initial mass (or density) of the clusters, and *(b)* the observed P2/P1 ratios most likely reflect their primordial values (i.e., there is no preferential loss of P1 stars, as suggested by some self-enrichment models).

2.2. *Observed Trends with Age*

Because light-element inhomogeneities were initially detected in clusters older than $\geq$ 10 Gyr, it has long been speculated that the formation of MPs was related to unique conditions present only in the early universe.

The first observational evidence of MPs in massive clusters with intermediate and younger ages (younger than approximately ∼6 Gyr) was provided by the HST survey led by Nate Bastian (e.g. Niederhofer et al. 2017; Hollyhead et al. 2017; Martocchia et al. 2018a, 2019). The detection of MPs in such young clusters leads to the conclusion that the conditions necessary for the formation of MPs are also present in the local universe (Martocchia et al. 2018a), suggesting a common pathway for the formation of GCs at both high and low redshifts (Pfeffer et al. 2018; Kruijssen et al. 2019). Specifically, this

https://doi.org/10.1017/S174392132500170X Published online by Cambridge University Press

corresponds to an age of $\sim$ 2 Gyr, which places the formation redshift at $z_{\rm formation} \sim 0.17$.

Due to their relatively young age, clusters around 2 Gyr offer a unique opportunity to constrain the occurrence of multiple bursts of star formation within the cluster. For example, in the case of NGC 1978, an analysis of sub-giant branch stars reveals that the two populations, which differ in their N abundances (normal and enhanced), are essentially coeval (Martocchia et al. 2018b). This finding places very stringent limits on the age difference between successive star formation events in a self-enrichment scenario. Furthermore, it challenges certain MP models that attribute self-enrichment to intermediate-mass stars, as such stars would require more time to enrich the cluster before the formation of the second generation.

Another key result from the survey of intermediate-age clusters is the correlation between the amplitude of the N spread and the cluster age (e.g. Martocchia et al. 2019). Specifically, the N spread is minimal in NGC 1978, which is 2 Gyr old, compared to older clusters. However, Martocchia et al. (2019) and Lagioia et al. (2019) reach different conclusions regarding the presence such an age trend for MPs. This discrepancy arises because the observed correlation is influenced by the clusters' metallicity and the evolutionary effects on N abundances. Specifically, N abundances in RGB stars are affected by the first dredge-up, which depends on the stars' mass and age. As a result, the N-rich star sequence converges with that of stars with normal N levels, causing the N spread to be underestimated. This phenomenon is more pronounced at younger ages (Salaris et al. 2020).

The challenge of interpreting photometric results for N has motivated efforts to confirm light-element variations by assessing their amplitude through chemical elements less influenced by evolutionary effects, such as Na. The first cluster studied in this context was, once again, NGC 1978. Saracino et al. (2020) utilised intermediate-resolution spectra obtained with MUSE, combining them based on photometric classification into two representative spectra: one for the population with standard N levels and another for the population with enhanced N. Their analysis revealed that these two groups also exhibit differences in Na abundances, with a modest spread of approximately 0.07 dex between them. The same approach was applied to two additional, older clusters, where observed Na variations were on the order of 0.20 dex. These variations are larger than those found in NGC 1978 but smaller than those observed in older Galactic clusters with similar metallicity (Martocchia et al. 2020). Collectively, these results suggest that the chemical differences between sub-populations may increase with cluster age. However, larger spectroscopic samples are required to confirm this finding.

So far, MPs have not been detected among evolved stars in globular clusters younger than approximately 1.5 Gyr (Mucciarelli et al. 2008, 2014; Cabrera-Ziri et al. 2016; Lardo et al. 2017). However, it remains uncertain whether this absence reflects a true lack of MPs in these clusters or if they are simply undetectable in more massive stars using current observational techniques.

For example, as discussed earlier, mixing effects from the first dredge-up can homogenise initial N abundance differences between P1 and P2 stars on the RGB, particularly in younger clusters. To address this, the current focus has shifted to detecting photometric spreads on the main sequence (MS), where N abundances remain unaffected by evolutionary processes. This approach has been successfully applied to NGC 1783, currently the youngest cluster known to host MPs. In this cluster, a small N spread of only 0.3 dex was observed among MS stars (Cadelano et al. 2022).

As a second example, prior to the discovery of N variations from HST photometry and Na variations from MUSE spectra, NGC 1978 had been studied using high-resolution spectroscopy and integrated spectroscopy. In both cases, it was concluded that the

https://doi.org/10.1017/S174392132500170X Published online by Cambridge University Press

observed sodium spread was consistent with observational errors. Notably, the extremely small Na variation measured by Saracino et al. (2020) would be difficult to detect through integrated spectroscopy or high-resolution spectra, especially in cases where the signal-to-noise ratio is low, as is common in distant stellar systems. Overall, this highlights the importance of differential spectroscopy for mitigating systematic errors and uncovering subtle abundance differences in young clusters.

3. Some Interesting Recent Developments

3.1. *Supernova Avoidance and Duration of Star Formation*

Cluster formation is ultimately terminated by feedback processes, which, for the most massive clusters, involve a variety of mechanisms. Studies examining gas expulsion and the cessation of star formation (SF) have often assumed that all stars above 8 $M_\odot$ end their lives as CCSNe (e.g., Wirth et al. 2022). However, recent findings indicate that particularly massive stars (> 30 $M_\odot$) often fail to explode, instead collapsing into black holes as *failed CCSNe*. While results show some variability, it has been consistently demonstrated that stars up to 20 $M_\odot$ predominantly explode as CCSNe, while stars with higher masses are more likely to undergo failed CCSNe (e.g., Heger et al. 2003).

In this context, Wirth et al. (2024) examined SF durations under the assumption that all stars above 20 $M_\odot$ result in failed CCSNe. They found that a SF duration of $\sim$3.5 Myr, assuming all stars above 8 $M_\odot$ explode as CCSNe (Wirth et al. 2022), would translate into an upper limit of $\sim$10.5 Myr when accounting for the impact of failed CCSNe. This difference has significant implications for GC formation, as longer SF durations would allow for extended periods of pollution from binary systems and stellar winds from massive stars, facilitating the formation of MPs (e.g., de Mink et al. 2009; Sills et al. 2010; Gieles et al. 2018; Renzini et al. 2022; Nguyen et al. 2024).

To further enhance our understanding of SF durations, it is essential to investigate the nature of CCSNe, particularly how factors such as stellar initial mass, metallicity, and rotation influence iron ejection. Additionally, studying the distribution of stellar rotation in young GCs is crucial, as rotation significantly affects both the amount and the chemical composition of ejecta (Limongi & Chieffi 2018).

3.2. *Formation of Massive Star Clusters in Giant Molecular Clouds*

The widespread presence of MPs in GCs across a broad range of ages, metallicities, and masses suggests that MPs may be a natural outcome of the formation process in the most massive clusters. Building on this premise, Howard et al. (2019) explored whether MPs with realistic properties could arise within the standard framework of cluster formation. Their study employed 3D radiative hydrodynamics simulations to model the formation of massive star clusters within giant molecular clouds (GMCs) of 10^7 $M_\odot$ (Howard et al. 2018).

By using He abundance as a tracer for enrichment, Howard et al. (2019) demonstrated that MP characteristics could emerge when He enrichment accounts for a few percent of the cluster's total mass. Furthermore, variations in individual formation histories lead to diverse P1/P2 distributions, reproducing the natural variability in MP properties.

In these simulations, massive clusters form rapidly—within approximately 5 Myr—through a combination of gas accretion from natal GMC filaments and mergers with proto-clusters. This model effectively resolves the *mass budget* problem by embedding cluster growth within GMCs rather than treating clusters as isolated gas clouds. Indeed, young clusters access the gas reservoir of the GMC through filamentary inflows, enabling sustained growth and prolonged star formation.

https://doi.org/10.1017/S174392132500170X Published online by Cambridge University Press

3.3. *Candidate Stellar Polluters*

In the study of MPs, the focus on stellar polluters has evolved over time. While AGBs have received considerable attention in the past, the current trend is shifting toward exploring winds from massive stars and interacting binaries (IBs). This change is driven by the rapid evolution of these stellar sources, which ensures the timely release of enriched material necessary for the formation of P2 stars, well matching observations.

Given that nearly all massive stars form in binaries or higher-order systems, particularly in dense clusters, IBs naturally emerge as significant contributors to the enriched material required for MP formation. Additionally, IBs offer a highly promising avenue due to the extensive parameter space they occupy. Recently, Nguyen et al. (2024) introduced a comprehensive grid of over 200 IB models, exploring variations in primary mass, period, and mass ratio at a metallicity of [Fe/H] = –1.4. Their study demonstrates that massive binaries can eject up to 23% of their mass in material with the appropriate composition to match the P2 stars. This enrichment occurs within approximately 12 Myr, a timescale that aligns more closely with current observational constraints compared to many alternative scenarios.

Another promising category of stellar polluters is very massive stars (VMSs), with masses reaching several hundred solar masses ($\sim 10^2 M_\odot$). Higgins et al. (2023) modelled stars in the range of 50-500 $M_\odot$ at solar metallicity to assess their potential role in explaining the abundance patterns observed in GC stars. Their findings indicate that VMSs can enrich their stellar winds with elements processed through hot CNO burning far more effectively than their lower-mass counterparts. For instance, a 200 $M_\odot$ star ejects 100 times more of each heavy element in its winds compared to a 50 $M_\odot$ star†.

While the mass budget problem is not fully resolved, the contributions of VMSs significantly mitigate the issue. Together with IBs, VMSs present a compelling case for their combined role in explaining the enriched chemical abundance patterns observed in GCs (Renzini et al. 2022; Lahén, Naab, & Szécsi 2024).

3.4. *Hints from High-z Observations*

Globular clusters' old ages ($\geq$ 10 Gyr) and small radii ($\sim$ few pc) have long precluded direct observations of their formation. However, a breakthrough has emerged from the realm of strong gravitational lensing, allowing the observation of star formation at high redshifts on extremely small physical scales. This has opened a window into the formation phases of (proto-)GCs (e.g., Cava et al. 2018).

Notably, observational studies (e.g., Vanzella et al. 2017, 2019) have utilized lensing amplification in distant galaxy clusters ($z \sim 2$–6) to identify compact objects with sizes and masses consistent with proto-GCs—essentially, GCs in the early stages of their formation. With the capabilities of the James Webb Space Telescope (JWST), spectroscopy and imaging of large numbers of such objects at high redshift are now possible, providing the opportunity to assess whether they are indeed GCs and investigate their properties (Vanzella et al. 2021, 2022; Mowla et al. 2022, 2024; Harris & Reina-Campos 2023; Claeyssens et al. 2023; Adamo et al. 2023; Forbes & Romanowsky 2023).

Despite the challenges in interpreting high-redshift data—such as uncertainties in the initial mass function, stellar population models, lens stretching, and confusion with cluster complexes, nuclear star clusters, and ultra-compact dwarf galaxies (see the interesting discussion in Pfeffer et al. 2025)—the observation of high-redshift GC candidates opens the possibility of uncovering the elusive formation of GCs and their MPs in the first few Gyr.

† Even when weighted by the initial mass function, the wind contribution from VMSs remains an order of magnitude higher than that of lower-mass stars (Higgins et al. 2023).

https://doi.org/10.1017/S174392132500170X Published online by Cambridge University Press

4. Conclusions

Once considered a niche topic, the study of GCs and their MPs has gained significant attention, particularly with the discovery of clusters forming in the distant universe through JWST. These observations offer a unique perspective on MP formation while underscoring the need for a deeper understanding of MP properties in resolved star clusters to accurately interpret integrated light.

Observational evidence has also conclusively shown that even younger clusters exhibit variations in light elements similar to those in older clusters, suggesting that star clusters in both low- and high-redshift galaxies may form via common mechanisms. This insight has opened new research avenues that could refine models and provide fresh constraints on the origins of MPs.

Although current models have yet to fully catch up with observational progress, several attempts to simulate the initial conditions of GC formation and evolution have shown promising results. These advancements suggest that understanding the origin of MPs requires collaboration across fields. Experts in local and high-redshift observations, as well as simulations, must work together, approaching the problem from multiple perspectives.

This review was presented at the IAU Symposium 395: *Stellar Populations in the Milky Way and Beyond*, a symposium held in honour of Beatriz Barbuy's life and work. Prof. Barbuy's contributions to the study of stellar populations were both foundational and far-reaching. The stories shared by many friends and colleagues who attended the symposium deepened my appreciation for her exceptional scientific rigour and mentoring skills. What stood out was her distinctive propensity for collaboration, a hallmark that not only defined her approach but also anticipates the direction modern astrophysics is taking.

References

Adamo *et al.*, 2023, *MNRAS*, 525, L6.
Bastian & Lardo 2018, *ARA&A*, 56, 83–136.
Bastian & Lardo 2015, *MNRAS*, 453, 357–364.
Bonatto *et al.*, 2019, *A&A*, 622, A179.
Cabrera-Ziri *et al.*, 2016, *MNRAS*, 460, 1869–1875.
Cadelano *et al.*, 2022, *ApJl*, 924, L2.
Cava *et al.*, 2018, *NatAs*, 2, 76.
Charbonnel C., 2016, *EAS*, 80–81, 177.
Claeyssens *et al.*, 2023, *MNRAS*, 520, 2180.
Carretta, *et al.*, 2009, *A&A*, 505, 117–138.
Carretta, *et al.*, 2010, *A&A*, 516, A55.
Conroy 2012 *ApJ*, 758, 21.
Decressin, *et al.*, 2007, *A&A*, 464, 1029–1044.
D'Antona, *et al.*, 2016, *MNRAS*, 458, 2122–2139.
D'Ercole, *et al.*, 2010, *MNRAS*, 407, 854-869.
de Mink, *et al.*, 2009, *A&A*, 507, L1–L4.
Forbes & Romanowsky, 2023, *MNRAS*, 520, L58.
Gratton, Sneden, Carretta 2004, *ARA&A*, 42, 385–440.
Gratton, Carretta, Bragaglia 2012, *A&ARv*, 20, 50.
Gratton, *et al.*, 2019, *A&ARv*, 27, 8.
Harris & Reina-Campos M., 2023, *MNRAS*, 526, 2696.
Heger *et al.*, 2003, *AJ*, 591, 288.
Higgins *et al.*, 2023, *MNRAS*, 526, 534.
Hollyhead *et al.*, 2017, *MNRAS*, 465, L39–L43.

https://doi.org/10.1017/S174392132500170X Published online by Cambridge University Press

Howard, Pudritz, Harris 2018, *Nature Astronomy*, 2, 725–730.
Howard, *et al.*, 2019, *MNRAS*, 486, 1146–1155.
Ivans *et al.*, 2001, *AJ*, 122, 1438.
Gieles, *et al.*, 2018, *MNRAS*, 478, 2461–2479.
Kader *et al.*, 2022, *ApJ*, 940, 76.
Kraft *et al.*, 1995, *AJ*, 109, 2586.
Kruijssen 2015 *MNRAS*, 454, 1658–1686.
Kruijssen *et al.*, 2019, *MNRAS*, 486, 3134–3179.
Lagioia *et al.*, 2019, *AJ*, 158, 202.
Lahén, Naab, Szécsi, 2024, *MNRAS*, 530, 645.
Lardo *et al.*, 2017, *MNRAS*, 468, 2482–2488.
Lardo *et al.*, 2018, *A&A*, 616, A168.
Lardo, *et al.*, 2022, *A&A*, 662, A117.
Lardo, *et al.*, 2023, *A&A*, 669, A19.
Larsen, Strader, Brodie 2012, *A&A*, 544, L14.
Larsen *et al.*, 2014, *ApJ*, 797, 15.
Limongi & Chieffi, 2018, *ApJS*, 237, 13.
Legnardi, *et al.*, 2022, *MNRAS*, 513, 735–751.
Marino, *et al.*, 2012, *A&A*, 541, A15.
Marino, *et al.*, 2019, *MNRAS*, 487, 3815–3844.
Marino *et al.*, 2019, *ApJ*, 887, 91.
Martocchia *et al.*, 2018, *MNRAS*, 473, 2688–2700.
Martocchia *et al.*, 2018, *MNRAS*, 477, 4696.
Martocchia *et al.*, 2019, *MNRAS*, 487, 5324–5334.
Martocchia *et al.*, 2020, *MNRAS*, 499, 1200.
Milone, *et al.*, 2015, *ApJ*, 808, 51.
Milone, *et al.*, 2017, *MNRAS*, 464, 3636–3656.
Milone *et al.*, 2018, *MNRAS*, 481, 5098–5122.
Milone & Marino, 2022, *Universe*, 8, 359.
Masseron, *et al.*, 2019, *A&A*, 622, A191.
Mészáros, *et al.*, 2015, *AJ*, 149, 153.
Mucciarelli *et al.*, 2008, *AJ*, 136, 375–388.
Mucciarelli *et al.*, 2014, *ApJl*, 793, L6.
Monelli *et al.*, 2013, *MNRAS*, 431, 2126–2149.
Mowla *et al.*, 2022, *ApJL*, 937, L35.
Mowla *et al.*, 2024, *Natur*, 636, 332. doi:10.1038/s41586-024-08293-0.
Niederhofer *et al.*, 2017, *MNRAS*, 464, 94–103.
Nguyen, Sills, 2024, *ApJS*, 237, 13.
Piotto, G., *et al.*, 2015, *AJ*, 149, 91.
Pancino, E., *et al.*, 2017, *A&A*, 601, A112.
Pfeffer, J., *et al.*, 2018, *MNRAS*, 475, 4309–4346.
Pfeffer, J., *et al.*, 2025, *MNRAS*, 536, 1878.
Portegies Zwart, S., McMillan, S., & Gieles, M., 2010, *ARA&A*, 48, 431.
Reina-Campos, M., *et al.*, 2018, *MNRAS*, 481, 2851–2857.
Renzini, A., 2008, *MNRAS*, 391, 354–362.
Renzini, A., *et al.*, 2015, *MNRAS*, 454, 4197–4207.
Renzini, A., 2017, *MNRAS*, 469, L63–L67.
Renzini, A., Marino, A., & Milone, A., 2022, *MNRAS*, 513, 2111–2117.
Salaris, M., *et al.*, 2020, *MNRAS*, 492, 3459.
Saracino, F., *et al.*, 2020, *MNRAS*, 498, 4472.
Sarajedini, A., *et al.*, 2007, *AJ*, 133, 1658.
Schiavon, R. P., *et al.*, 2013, *ApJL*, 776, L7.
Schiavon, R. P., *et al.*, 2017, *MNRAS*, 465, 501–524.
Schiavon, R. P., *et al.*, 2024, *MNRAS*, 528, 1393–1407.

https://doi.org/10.1017/S174392132500170X Published online by Cambridge University Press

Sills, A., & Glebbeek, E., 2010, *MNRAS*, 407, 277–284.
Soto, M., *et al.*, 2017, *AJ*, 153, 19.
Sneden, C., *et al.*, 2004, *AJ*, 127, 2162.
Sneden, C., Pilachowski, C. A., & Kraft, R. P., 2000, *AJ*, 120, 1351.
Stetson, P. B., *et al.*, 2019, *MNRAS*, 485, 3042–3063.
Vanzella, E., *et al.*, 2017, *ApJ*, 842, 47.
Vanzella, E., *et al.*, 2019, *MNRAS*, 483, 3618.
Vanzella, E., *et al.*, 2021, *A&A*, 646, A57.
Vanzella, E., *et al.*, 2022, *ApJL*, 940, L53.
Wirth, V., *et al.*, 2022, *MNRAS*, 516, 3342–3353.
Wirth, V., *et al.*, 2024, *A&A*, 691, A227.
Yong, D., *et al.*, 2008, *ApJ*, 684, 1159.

https://doi.org/10.1017/S174392132500170X Published online by Cambridge University Press